

MYC regulation of a “poor-prognosis” metastatic cancer cell state

Anita Wolfer^{a,b,1}, Ben S. Wittner^{a,b,1}, Daniel Irimia^{b,c,d}, Richard J. Flavin^{b,e}, Mathieu Lupien^{b,f,2}, Ruwanthi N. Gunawardane^{b,3}, Clifford A. Meyer^g, Eric S. Lightcap^h, Pablo Tamayoⁱ, Jill P. Mesirovⁱ, X. Shirley Liu^g, Toshi Shioda^{a,b}, Mehmet Toner^{b,c,d}, Massimo Loda^{b,e,i}, Myles Brown^{b,f}, Joan S. Brugge^{b,i,4}, and Sridhar Ramaswamy^{a,b,i,j,4}

^aMassachusetts General Hospital Cancer Center, Boston, MA 02114; ^bHarvard Medical School, Boston, MA 02115; ^cCenter for Engineering in Medicine, Massachusetts General Hospital/East, Charlestown, MA 02129; ^dShriners Hospital for Children, Boston, MA 02114; ^eCenter for Molecular Oncologic Pathology, Dana-Farber Cancer Institute, Boston, MA 02115; ^fDepartment of Medical Oncology, Dana-Farber Cancer Institute, Boston, MA 02115; ^gHarvard School of Public Health, Boston, MA 02115; ^hMillennium Pharmaceuticals, Inc., Cambridge, MA 02139; ⁱBroad Institute, Cambridge, MA 02142; and ^jHarvard Stem Cell Institute, Cambridge, MA 02138

Contributed by Joan S. Brugge, December 18, 2009 (sent for review November 3, 2009)

Gene expression signatures are used in the clinic as prognostic tools to determine the risk of individual patients with localized breast tumors developing distant metastasis. We lack a clear understanding, however, of whether these correlative biomarkers link to a common biological network that regulates metastasis. We find that the c-MYC oncoprotein coordinately regulates the expression of 13 different “poor-outcome” cancer signatures. In addition, functional inactivation of MYC in human breast cancer cells specifically inhibits distant metastasis in vivo and invasive behavior in vitro of these cells. These results suggest that MYC oncogene activity (as marked by “poor-prognosis” signature expression) may be necessary for the translocation of poor-outcome human breast tumors to distant sites.

breast cancer | biomarkers | invasion and migration | transcriptional profiling

Over the past decade, 13 different multigene “poor-outcome” cancer signatures have been identified using DNA microarray-based gene expression profiling (1–12). Quantitative increases in the expression of these different signatures within a primary tumor are correlated with its likelihood of metastasis to distant sites across a spectrum of different solid tumor types (Fig. 1A). Some of these prognostic signatures, including the 21-gene Oncotype Dx and 70-gene MammaPrint gene sets, were derived from breast tumors and have been deployed as biomarkers for risk stratification in patients with newly diagnosed breast cancer (6, 9–11). However, many other such signatures were originally derived using a variety of experimental approaches, have individually been associated with varying aspects of cancer progression (i.e., transformation, proliferation, dedifferentiation/stemness, genetic instability, and metastasis), are prognostic in malignancy beyond breast cancer, and appear to overlap minimally with respect to component genes (Fig. S1 and Table S1). Thus, whether these 13 different signatures as a set link to a common biological network related to metastasis remains unclear.

Results

Although these 13 “poor-prognosis” signatures were derived in various ways, many without any relation to breast cancer, most are prognostic across different breast tumor expression data sets. A few of these signatures also are coordinately expressed in the same high-risk human breast tumors (13). Importantly, many poor-prognosis signatures contain genes whose expression correlates with estrogen receptor (ER) status in breast cancer, and estrogen signaling is known to drive the growth and survival of breast cancer cells from the earliest stages of disease (14). These observations led to the hypothesis that estrogenic signaling may regulate the expression of both signatures derived from breast tumors and other diverse signatures derived in non-breast cancer contexts. To test this hypothesis, we assayed the expression of the 13 poor-outcome tumor

signatures using Affymetrix microarrays in estrogen-dependent ER α^+ / β^- MCF7 breast cancer cells after experimental manipulation of estrogenic signaling (15).

Detailed statistical analysis revealed that a significant proportion of genes in each of these 13 different transcriptional signatures was indeed expressed by MCF7 cells and was tightly and coordinately regulated by signaling through the ER (Fig. 1B, Figs. S2 and S3, and Table S2). Different signatures overlapped by no more than 10% with respect to individual component genes (Fig. S1). Furthermore, even this minimal overlap between different signatures could not account for the coordinate pattern that we observed, which was far beyond chance based on permutation analysis using both random and unrelated, experimentally derived signature sets (Table S3). Overall, approximately 40% of all poor-outcome signature genes were estrogen-regulated in MCF7 cells, with proportions in individual signatures ranging from around 30% to nearly 100% (Table S2). These initial findings in a cancer cell–autonomous experimental system demonstrated that the ER can functionally regulate the coordinate expression of a majority of poor-prognosis signatures.

Beyond ER, we also observed similar transcriptional effects with other oncogenes. For example, ERBB2 overexpression and EGF stimulation in MCF10A breast epithelial cells, which are immortalized but untransformed, both induced coordinated expression of all 13 poor-outcome signatures (Fig. 1C and D), and stimulation of LNCaP prostate cancer cells with dihydrotestosterone (DHT) via the androgen receptor (AR) produced a similar transcriptional pattern, albeit somewhat more weakly than ERBB2 or EGF signaling with respect to the “DOWN” metagenes from different signatures (Fig. 1E). These results suggested that increased activity of four different oncogenic pathways known to independently regulate cancer cell growth and survival in different cellular contexts could push different epithelial cell types toward a common transcriptional state defined by the coordinate expression of 13 different poor-outcome signatures.

Author contributions: A.W., B.W., D.I., and S.R. designed research; A.W., B.W., D.I., R.F., and E.S.L. performed research; D.I., R.N.G., T.S., M.T., M.B., and J.S.B. contributed new reagents/analytic tools; A.W., B.W., D.I., R.F., M. Lupien, C.A.M., P.T., J.P.M., X.L., M. Loda, M.B., J.S.B., and S.R. analyzed data; and A.W., B.W., and S.R. wrote the paper.

The authors declare no conflict of interest.

Data deposition: The microarray data reported in this paper have been deposited in the Gene Expression Omnibus (GEO) database, www.ncbi.nlm.nih.gov/geo. For a list of accession numbers, see Table S5.

¹A.W. and B.S.W. contributed equally to this work.

²Present address: Norris Cotton Cancer Center, Dartmouth Medical School, Lebanon, NH 03756.

³Present address: Ambit Biosciences, San Diego, CA 92121.

⁴To whom correspondence may be addressed. E-mail: sridhar@mgh.harvard.edu or joan_brugge@hms.harvard.edu.

This article contains supporting information online at www.pnas.org/cgi/content/full/0914203107/DCSupplemental.

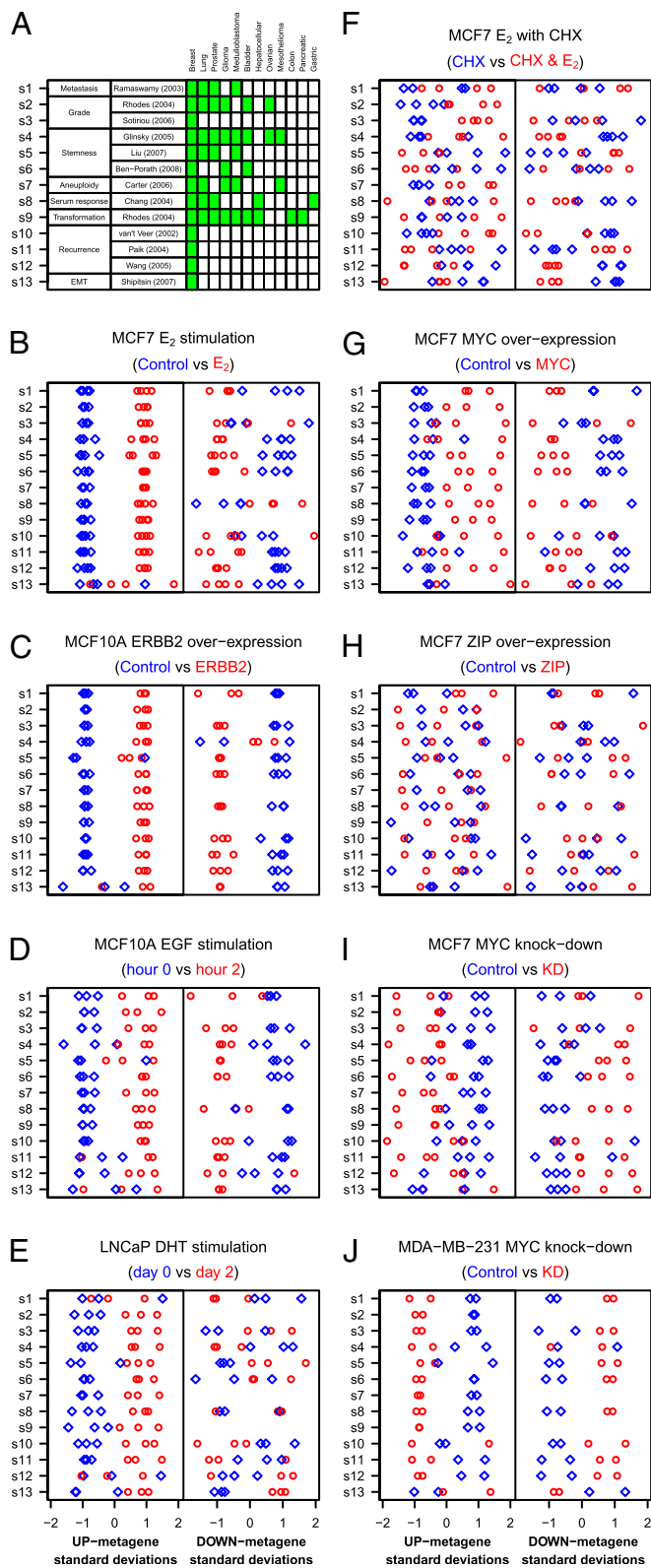


Fig. 1. Molecular regulation of 13 poor-outcome human cancer signatures. (A) Thirteen different signatures (designated s1–s13), correlated with different biological processes associated with metastatic progression, reported to be prognostic in different tumor types (green). To simplify the analysis, we first created two “metagenes” by separately averaging up-regulated and down-regulated genes from each multigene poor-outcome cancer signature (s1–s13). (B–J) Plots displaying UP and DOWN metagenes derived from each signature in standard deviation units after (B) 17 β -estradiol stimulation from

We next investigated whether poor outcome signature regulation reflected direct or indirect effects of these oncogenes on transcription. ERBB2 and EGFR, as membrane-bound receptor tyrosine kinases, almost certainly induced poor-outcome signature expression indirectly by signaling through downstream transcription factors. In contrast, ER α and AR are nuclear hormone receptors whose transcriptional activity can be modulated by the EGFR and ERBB2 pathways, raising the possibility that these transcription factors might directly regulate poor-outcome signature expression. But treatment of MCF7 cells with 17 β -estradiol in the presence of cycloheximide (CHX), a general inhibitor of new protein translation, destroyed coordinated signature induction by estrogen (Fig. 1F) (16). These results demonstrated that ER α might modulate poor-outcome signature expression indirectly, at least in part through a common transcriptional regulator downstream of the ER α , ERBB2, EGFR, and AR pathways.

Consequently, we analyzed the ER α -, ERBB2-, EGFR-, and AR-regulated transcriptional profiles in further detail, to identify candidate genes from the 13 poor-outcome signatures whose expression was commonly induced in response to these four different stimuli. Overall, approximately 50% of the poor-outcome signature genes were regulated by these different pathways across different cellular contexts. Although some poor-outcome genes were regulated uniquely by one of these pathways, others were commonly regulated by multiple pathways. In particular, ER α , ERBB2, EGFR, and AR commonly induced the expression of a “core gene set” of 20 poor-outcome genes, which was far beyond random ($P = 1.6 \times 10^{-12}$) (Fig. 2A).

Although this core gene set did not contain any obvious candidate transcriptional regulators, all of the genes in this set were linked into a single and highly-connected “core interactome” using the IPA algorithm and database of literature-based molecular interactions (Fig. 2B) (17). This core interactome was highly connected to the MYC transcription factor, which was not a member of any poor-outcome signature and thus was not in the core gene set itself. This correlation fit with the observation that at least 10 of 20 core interactome genes are known direct MYC targets (www.mycancer.org). It also was consistent with previous reports implicating MYC as a regulator of poor-prognosis signature expression in breast cancer (18–22). Taken together, this evidence raised the hypothesis that MYC, which is downstream of the ER α , ERBB2, EGFR, and AR pathways, may act as a common transcriptional regulator for expression of the 13 different poor-outcome signatures that we studied.

Consistent with this hypothesis, overexpression of MYC in MCF7 cells was sufficient to induce coordinated poor-prognosis signature expression (Fig. 1G) (23). In contrast, overexpression of ZIP (a MYC mutant lacking the two N-terminal transactivation domains) in MCF7 cells failed to induce this expression pattern (Fig. 1H). Furthermore, siRNA knockdown of endogenous MYC in MCF7 (ER⁺) reversed this coordinated pattern of signature expression (Fig. 1I) (24, 25). Overall, these transcriptional changes involved 20% of all poor-outcome signature genes in MCF7 cells, ranging

circles versus control (blue diamonds) in MCF7 cells, (C) ERBB2 over-expression (red circles) versus control (blue diamonds) in MCF10A cells, (D) EGF stimulation (red circles) versus control (blue diamonds) in MCF10A cells, (E) DHT stimulation (red circles) versus control (blue diamonds) in LNCaP cells, (F) 17 β -estradiol stimulation and CHX treatment (red circles) versus CHX treatment alone (blue diamonds) in MCF7 cells, (G) overexpression of MYC (red circles) versus vector control (blue diamonds) in MCF7 cells, (H) over-expression of ZIP (red circles) versus vector control (blue diamonds) in MCF7 cells, (I) siRNA knockdown of endogenous MYC (red circles) versus vector control (blue diamonds) in MCF7 cells, and (J) siRNA knockdown of endogenous MYC (red circles) versus vector control (blue diamonds) in MDA-MB-231 cells. Circles and diamonds represent independent replicates. s2, s7, and s9 are unidirectional signatures that have only up-regulated genes.

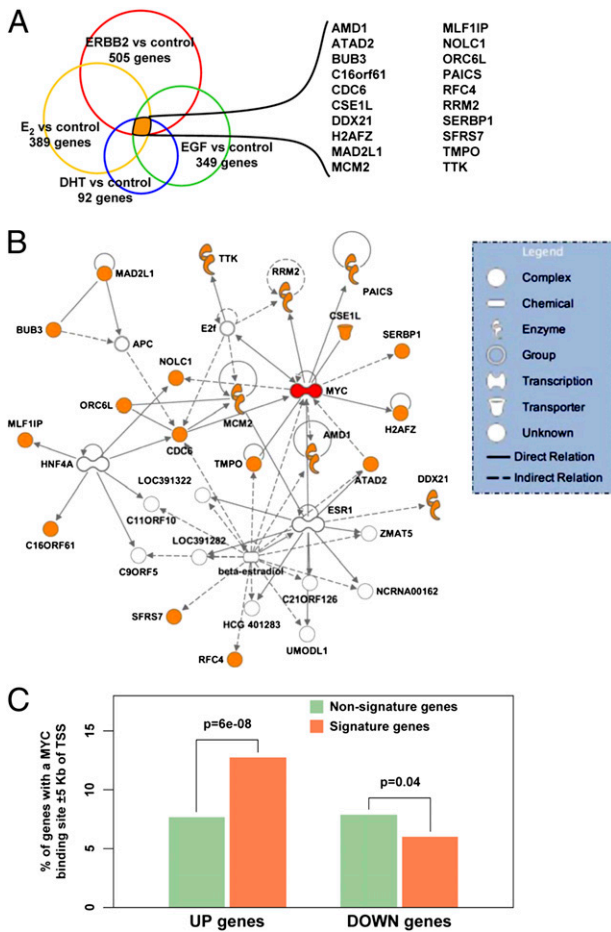


Fig. 2. MYC-centered core interactome. (A) Venn diagram illustrating derivation of the core gene set. (B) A highly connected network of the 20 genes in the core gene set (orange) and 13 associated genes identified using the IPA algorithm (17). MYC is highlighted in red. (C) Statistical analysis of genome-wide MYC-binding site data obtained from MCF7 cells after stimulation with 17 β -estradiol, generated using ChIP-Chip (chromatin immunoprecipitation and tiling microarrays spanning the entire nonrepetitive human genome) (26). UP and DOWN poor-outcome signature genes with at least one MYC binding site within ± 5 kb of their transcription start site (orange) versus the same for all other genes on the tiling array (green).

from 10% to 40% across individual signatures (Table S4). In addition, analysis of genome-wide MYC chromatin immunoprecipitation microarray (ChIP-Chip) profiling data, obtained from MCF7 cells after 17 β -estradiol treatment (26), demonstrated a highly significant enrichment for MYC binding within 5 kb of the transcriptional start sites of up-regulated poor-outcome signature genes ($P = 6 \times 10^{-8}$) (Fig. 2C). In contrast, we found no similar enrichment in MYC binding for down-regulated poor-outcome genes, suggesting that many down-regulated genes are in fact indirect MYC targets. Finally, siRNA knockdown of endogenous MYC in MDA-MB-231 (ER⁺PR⁺ERBB2⁻) breast cancer cells also reversed coordinated signature expression (Fig. 1J). These results demonstrated that MYC could powerfully regulate the coordinate expression of many, but not all, genes from 13 different poor-outcome transcriptional signatures in breast cancer cells.

MYC is known to regulate a wide spectrum of cancer cell behaviors, including proliferation, survival, differentiation, and genetic stability, which are general features of tumorigenesis (27). Therefore, one explanation for our findings was that MYC activity within cancer cells, as reflected by poor-prognosis signature expression, might indirectly influence the metastatic propensity of cancer cells (by, e.g.,

promoting cellular proliferation and survival). Another possibility was that MYC actually might regulate more specific aspects of metastatic cell behavior. To test this hypothesis, we focused on the MDA-MB-231 cell line, which is highly metastatic and stereotypically forms distant lung metastasis when injected into immunocompromised mice. This well-credentialed model has been used to experimentally identify and manipulate molecular pathways that regulate various aspects of metastatic cell behavior (28). Furthermore, MYC knockdown in these metastatic breast cancer cells resulted in the coordinate down-regulation of 13 different poor-outcome transcriptional signatures, supporting the relevance of this model system to human cancer metastasis (Fig. 1J). We therefore investigated whether inhibiting MYC activity would specifically inhibit the metastatic behavior of MDA-MB-231 cells.

Stable MYC knockdown with two different short-hairpin RNAs introduced using a lentiviral vector [hairpin 1 (HP1) $\approx 95\%$; hairpin 2 (HP2) $\approx 70\%$] did not significantly alter the growth kinetics of MDA-MB-231 cells after serial passage in vitro (Fig. 3A and B). It must be noted, however, that immediately after MYC knockdown, HP1 and HP2 cells did show mildly decreased proliferation that then normalized after 1–2 weeks of passage, suggesting that these cells depended on MYC for proliferation to some degree but were still able to preserve their proliferative drive in the face of stable MYC inhibition, presumably through compensatory changes. Importantly, stable MYC knockdown also did not significantly affect the kinetics of primary tumor formation after orthotopic injection into the mammary fat pad of immunocompromised NOD/SCID mice (Fig. 3C). Nine of 10 control mice and 8 of 10 experimental mice had similar-sized tumors 8 weeks after injection, whereas the remaining animals did not form tumors.

In contrast, MYC knockdown greatly inhibited the formation of distant lung metastasis (Fig. 3D). Whereas two animals had no lung metastases, four other animals had a small number of metastases compared with control animals at 8 weeks. One other MYC knockdown animal died of unknown causes at 5.5 weeks and so was not fully evaluable, but only had a small primary tumor and no signs of macroscopic metastasis at autopsy. Curiously, the last MYC knockdown animal was an outlier and was similar to animals in the control population in forming numerous lung metastases (Fig. 3D). To address this paradoxical finding, we examined MYC protein expression in the primary and metastatic tumors from this outlier by immunohistochemistry. Whereas the primary tumor was negative for MYC expression, confirming stable knockdown in cells at the point of orthotopic injection, metastatic cells in the lungs of this animal were strikingly positive for MYC expression, suggesting that rare cells had somehow reactivated MYC expression, enabling metastasis of these cells from the mammary fat pad to the lungs (Fig. 3E). Further histopathologic examination of primary tumors from MYC knockdown versus control animals revealed that both tumor types were high-grade carcinomas containing round polygonal cells with comparable levels of MKI-67, TUNEL, vimentin, and E-cadherin staining, which mark cell proliferation, apoptosis, and mesenchymal/epithelial cell state, respectively (Fig. 3F). Taken together, these in vivo results demonstrated that MYC activity was specifically required to maintain the metastatic state rather than the proliferative, apoptotic, or differentiation state of these highly metastatic breast cancer cells.

Given these findings in vivo, we finally examined whether MYC activity was necessary for fundamental and hallmark features of metastatic cell behavior, namely, cancer cell invasion and migration. We used a novel microfluidic device developed to study cell migration and invasion at the single-cell level, where locomotion is mechanically constrained along predefined paths (29). Each device contained an array of linear microcapillaries each 10 μ m tall, 20 μ m wide, and 600 μ m long. Individual MDA-MB-231 cells were visualized using live-cell time-lapse videomicroscopy after seeding into microcapillaries either filled with Matrigel (to simulate some of the three-dimensional microenvironmental

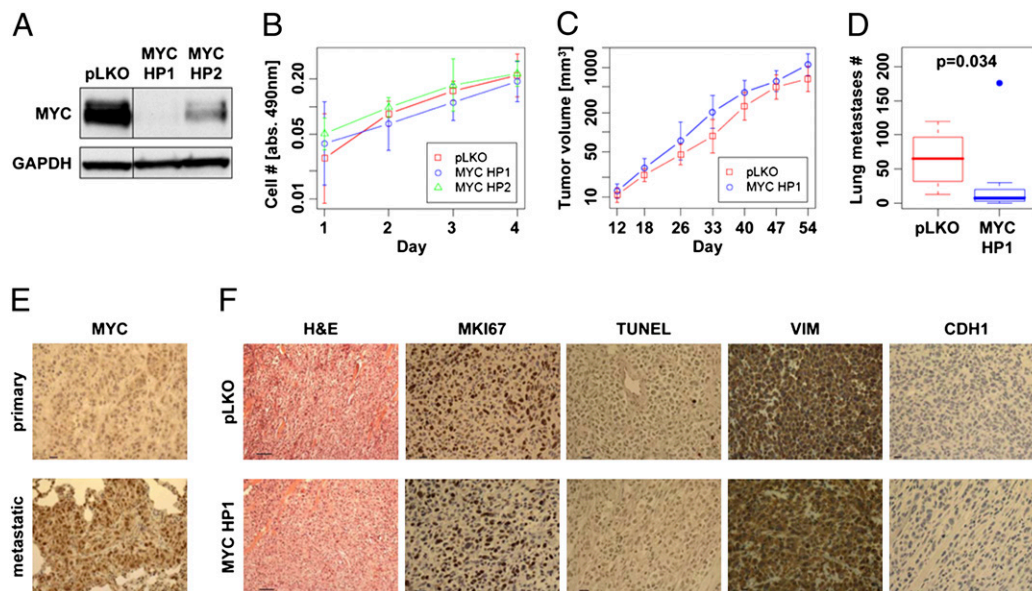


Fig. 3. MDA-MB-231 primary tumorigenesis and metastasis in vivo with stable MYC knockdown. (A) Western blot for MYC protein after stable, lentiviral-mediated knockdown with two different MYC hairpins (HP1 and HP2) compared with pLKO empty vector control after serial passage in MDA-MB-231 cells. (B) Proliferation curves for empty vector control (pLKO), HP1, and HP2 cells after serial passage over 4 days, showing absorbance as a measure of cell number ($n = 3$, 95% CI). (C) Tumor growth of control (pLKO) and HP1 cell xenografts in NOD/SCID mice (pLKO, $n = 9$; HP1, $n = 7$; 95% CI). (D) Boxplot of the number of lung metastases per mouse in control and MYC HP1 knockdown tumor-bearing mice (pLKO, $n = 9$; MYC HP1, $n = 7$; P value calculated from the two-sided, two-sample Wilcoxon test). (E) Representative immunohistochemistry for MYC protein expression in primary and metastatic tumor sections from the outlier animal in the MYC HP1 knockdown group. (F) Representative light microscopy (H&E) and immunohistochemistry (MKI67, TUNEL, vimentin, and e-cadherin) in pLKO control and MYC HP1 knockdown primary tumors. (Scale bars: 20 μm .)

conditions that cancer cells encounter in vivo) or simply coated with collagen IV (to study unimpeded migration). We specifically performed these experiments in the absence of a chemogradient, which allowed us to examine intrinsic cell behavior. Quantitative analysis of single-cell velocities in this device revealed that MYC knockdown greatly impeded MDA-MB-231 invasion in Matrigel but had only mild effects on migratory velocities compared with control cells (Fig. 4A–F, and Movies S1–S4). As was most evident in the time-lapse movies of migrating cells, however, knockdown cells were rounded, moved less efficiently and persistently, exhibited frequent and disordered changes in direction compared with control cells, and did not exit microcapillaries efficiently (Movies S3 and S4). We also assessed the quantitative effect of MYC knockdown on MDA-MB-231 cell invasion in more traditional Boyden chamber assays. We found that MYC knockdown in this experimental system led to a $\approx 50\%$ decrease in invasion (Fig. S4). These findings demonstrated that in highly metastatic MDA-MB-231 breast cancer cells, MYC is necessary to specifically maintain an invasive and migratory state.

Discussion

MYC is one of the most important somatically mutated oncogenes in human cancer. Recent studies suggest that inherited polymorphisms on 8q24 that powerfully modify solid tumor predisposition also influence MYC transcriptional regulation (30). Deregulation of the MYC oncoprotein confers a selective advantage on cancer cells in differing contexts by promoting proliferation, cell survival, differentiation blockade, epithelial to mesenchymal transition, and genetic instability, all of which can contribute to metastasis (27, 31–33). In fact, a recent report suggested that MYC functions as an indirect regulator of metastasis in a c-RAF-driven mouse model of non-small cell lung cancer by modulating growth, differentiation, and angiogenesis (34). MYC also has been implicated as a potentially important regulator of cancer stem cell growth and survival (22). Our findings add to these foundational observations by demonstrating that MYC activity also may be necessary for

cancer cell invasion, migration, and thus ultimately metastasis in certain contexts. In our experimental system, MYC's direct effects on invasion, migration, and metastasis are separate from its effects on survival, proliferation, and differentiation, presumably because of compensatory changes that maintain the proliferative drive of MDA-MB-231 cells after MYC knockdown in vitro and in vivo. To illustrate this point, MDA-MB-231 cells contain a mutation in KRAS that has been shown to maintain primary breast tumorigenesis in the setting of experimental MYC inactivation (35). In the natural human tumor setting, however, it seems likely that MYC coordinately regulates these many different cellular functions, which in combination are necessary for successful invasion, translocation, seeding, and growth at distant sites. Furthermore, whereas MYC activity is required for the invasive behavior of MDA-MB-231 cells, MYC overexpression in itself is not sufficient to induce invasion in noninvasive MCF10A cells, suggesting that other molecular pathways must cooperate with MYC to fully trigger the invasive phenotype during cancer progression (18, 36, 37). Further work is needed to precisely define the mechanisms through which MYC specifically regulates cancer cell translocation.

These results may partially explain why patients with early-stage primary tumors that express poor-prognosis transcriptional signatures are more likely to progress to distant metastasis. Previous work has focused mainly on prognostic signatures as genomic correlates of tumor proliferation, survival, and differentiation (9, 23, 38). Others have noted that four of the prognostic signatures in our analysis coordinately flag the same high-risk primary tumors (13). Moreover, independent groups have reported that (i) MYC regulates a few individual poor-outcome signatures in our analysis, (ii) a MYC-driven gene expression signature has prognostic value in primary human breast tumors, and (iii) poor-outcome signatures can be linked to MYC using alternative bioinformatic approaches (18–22). Consistent with these observations, we demonstrate that 13 different poor-prognosis cancer signatures, including the 70-gene MammaPrint and 21-gene Oncotype Dx biomarkers, coordinately reflect MYC activity within human breast cancer cells, that in turn is

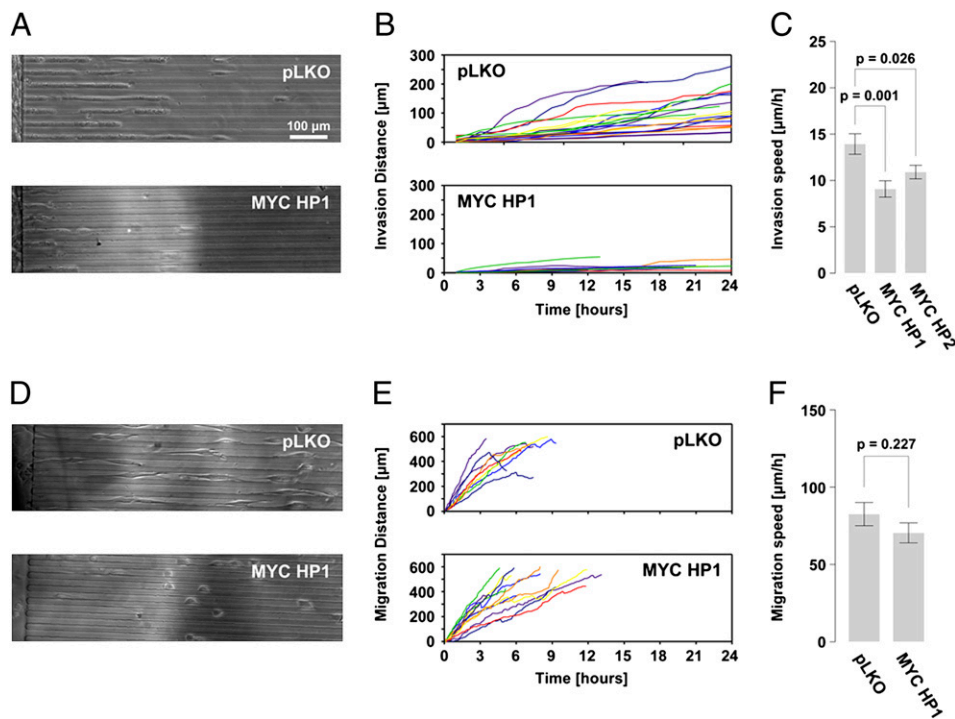


Fig. 4. MDA-MB-231 invasion and migration in vitro with stable MYC knockdown. (A) Representative light microscopy images of control (pLKO) and MYC knockdown (MYC HP1) MDA-MB-231 breast cancer cells migrating through Matrigel-filled microcapillaries. (B) Position of individual pLKO and MYC HP1 cells invading through Matrigel-filled microcapillaries over 24 h plotted against time. (C) Bar plot representing the average invasion speed through Matrigel for pLKO and MYC HP1 cells, $13.9 \pm 1.1 \mu\text{m/h}$ for pLKO ($n = 33$) and $9.1 \pm 0.9 \mu\text{m/h}$ for MYC HP1 ($n = 31$) and $10.9 \pm 0.7 \mu\text{m/h}$ for MYC HP2 ($n = 33$). *P* values were computed by the two-sided Walsh *t* test. (D) Representative light microscopy images of pLKO and MYC HP1 MDA-MB-231 breast cancer cells migrating through collagen IV-coated microcapillaries. (E) Position of individual pLKO and MYC HP1 cells migrating along collagen IV-coated microcapillaries over 12 h plotted against time. (F) Bar plot representing the average migration speed through collagen-coated microcapillaries for pLKO and MYC HP1 knockdown cells, $82.5 \pm 7.5 \mu\text{m/h}$ for pLKO ($n = 17$) and $70.4 \pm 6.4 \mu\text{m/h}$ for MYC HP1 ($n = 21$). *P* values were computed by the two-sided Walsh *t* test. Also see [Movies S1–S4](#).

required for their invasion and metastasis to distant sites. Increased MYC activity within human tumors presumably can be driven either by somatic mutation or by alterations in its myriad upstream regulatory pathways. This model is consistent with recent work demonstrating that the transition from in situ to invasive breast carcinoma within individual tumors is often associated with amplification of the MYC locus, which correlates with shorter metastasis-free and overall survival and is an independent prognostic factor in multivariate analysis of clinical outcome (39, 40). Finally, many of the poor-outcome signatures in our analysis have prognostic value in other solid tumor types in which MYC deregulation is known to occur. This raises the possibility that MYC may in fact be generally necessary for the invasion, migration, and metastasis of other human solid tumor types beyond breast cancer.

Materials and Methods

More detailed information is available in [SI Methods](#).

Cross-Platform Gene Mapping. Data sources, in priority order, were the “best” versions of the Array Comparison Spreadsheets available on the Affymetrix website, Affymetrix annotation files for the appropriate array (version na24), UniGene file Hs.data (build 209), Entrez file gene2accession.gz (downloaded February 3, 2008), and [www.rii.com/publications/data/Array-Nomenclature_contig_accession.xls](#) (downloaded February 2, 2008). See [SI Methods](#) for more details.

Derivation and Statistical Significance of the Core Gene Set. For each of Fig. 1 *B–E*, the set of genes regulated by the corresponding experiment was determined as follows. For each probe set from each of the 13 signatures, the pooled-variance *t*-statistic was computed so that red samples higher than blue would yield a positive *t*-statistic. A one-sided *P* value was then defined as $P(t > T)$ for an UP probe set and as $P(t > -T)$ for a DOWN probe set, where *t* is drawn from a *t* distribution with $n - 2$ degrees of freedom and n is the number of samples in the experiment. The *P* values were then adjusted by the method of Benjamini and Hochberg (41), and a threshold was chosen to limit the false discovery rate to 5%. The probe sets below the threshold were then mapped to Entrez GeneIDs as described above. The resulting individual four sets of genes (corresponding to experiments shown in Fig. 1 *B–E*) were intersected to form the core gene set. The statistical significance of this observed intersection was defined to be the probability of randomly getting an intersection of size equal to or greater than

that of the core gene set. The computation of this probability is described in [SI Methods](#).

Network Analysis Using the IPA Algorithm and Database. Network analysis using the IPA algorithm and database was performed as described previously (17).

Gene Expression Profiles. Gene expression data from the following references were analyzed: 17 β -estradiol treatment of MCF7 cells with and without pretreatment with cycloheximide (16), MYC and ZIP overexpression in MCF7 cells (42), and knockdown of MYC in MCF7 and MDA-MB-231 cells (24). Gene expression profiles for MCF10A cells were obtained by transducing the cells with retroviruses encoding vector control (pBabe) or pBabe-ErbB2 (obtained from Danielle Carroll), using polybrene as described previously (43). After infection, cells were switched to assay medium supplemented with only 2% horse serum without EGF. For EGF stimulation, MCF10A cells transduced with empty vector were treated with 50 ng/mL EGF for 2 h before harvesting. All cells were harvested for RNA extraction 26 h after infection. Expression microarrays were Affymetrix U133Plus2.0. Gene expression profiles of LNCaP cells upon androgen stimulation were obtained by maintaining LNCaP cells in phenol red-free RPMI supplemented with 10% charcoal/dextran-stripped FCS for 3 days before stimulation with 100 nM DHT for 48 h. Expression microarrays were Affymetrix U133Plus2.0.

MYC Knockdown in MDA-MB-231 Cells. MDA-MB-231 breast cancer cells were purchased from American Type Culture Collection and maintained in DMEM–10% FCS at 37 °C and 5% CO₂. Cells were infected with lentivirus encoding either empty pLKO vector or pLKO containing one of two different hairpins against MYC (MYC HP1: TRCN0000174055; MYC HP2: TRCN0000010390). After 24 h of infection, the cells were selected in puromycin for 48 h and passaged for 2 weeks, after which target knockdown was assessed by Western blot analysis (Cell Signaling Technology). Films were scanned and knockdown was estimated, normalized to GAPDH using the National Institutes of Health’s ImageJ software.

Cellular Proliferation. Control (pLKO) and MYC knockdown (MYC HP1 and HP2) MDA-MB-231 cells were seeded at 10^3 cells/well in a 96-well plate in triplicate. Cell numbers were measured using the CellTiter 96 Aqueous One Solution Cell Proliferation Assay (Promega). The experiment was repeated three times.

In Vivo Metastasis Assay. Cells were harvested at 60–70% confluence using trypsin, and then counted and washed twice in PBS and resuspended in HBSS/30% Matrigel (BD Biosciences). The cells (1.5×10^6) were injected s.c.

over the nipple of 4-week-old female NOD/SCID mice (Jackson Laboratory). Tumors were measured weekly by caliper, and the mice were killed 8 weeks after tumor injection. Tumors and lungs were collected, fixed, and stained. H&E slides of formalin-fixed, paraffin-embedded material were used to assess the morphological integrity and geographical variation in morphology of tissue samples, as well as count the number of lung metastases. Lung metastases were defined as tumor cell clusters ≥ 1 mm in size and morphologically identical to the primary tumor. Indirect immunoperoxidase analysis was performed on tumors for Ki67 (M7240, diluted 1:1,000; Dako) and c-Myc (1472-1, diluted 1:50; Epitomics). The APOPTAG Apoptosis Kit (Millipore) was used for indirect TUNEL staining. Each tissue section was evaluated by a board-certified pathologist (R.F.). Mouse experiments were carried out under a Massachusetts General Hospital Institutional Review Board–approved protocol.

Invasion and Migration Assays. Microcapillary arrays were fabricated as described previously (29). Immediately after bonding, and while the PDMS was still hydrophilic, devices were coated with either Matrigel or collagen IV. Within a few hours after device fabrication, 2 μ l of cell suspension was loaded in the device at

10^6 – 10^7 cells/ml, and individual wells on the plate were filled with 3 ml of media (DMEM/10% FCS), completely covering the microfluidic devices. The multiwell plate was mounted on the automated stage of an Zeiss Axiovert microscope equipped with an environmental chamber set at 37 °C and 5% CO₂. Cells were imaged using a 10 \times objective and phase contrast with individual frames acquired from three different locations of each device every 6 min for 24–72 h.

ACKNOWLEDGMENTS. We thank Daniel Haber, Nick Dyson, and Nabeel Bardeesy for discussions and advice and Kat Coser, Ipsita Dey-Guha, Giuseppe Fedele, and Giorgia Zadra for technical assistance. This work was supported by the National Cancer Institute (Grants K08 CA100339 and P50 CA89393, to S. R.), the Richard & Susan Smith Family Foundation (a New Investigator Award to S.R.), the Howard Hughes Medical Institute (Physician-Scientist Early Career Award to S.R.), the Sidney Kimmel Foundation (Translational Science Award to S.R.), the Breast Cancer Research Foundation (J.S.B.), the Susan G. Komen Foundation (Grants FAS0703860 and KG0905151, to T.S.), U.S. Department of Defense (Award DAMD17-03-1-0408, to R.N.G.), the Swiss National Science Foundation (A.W.), and the Emma Muschamp Foundation (A.W.).

- Ben-Porath I, et al. (2008) An embryonic stem cell–like gene expression signature in poorly differentiated aggressive human tumors. *Nat Genet* 40:499–507.
- Carter SL, Eklund AC, Kohane IS, Harris LN, Szallasi Z (2006) A signature of chromosomal instability inferred from gene expression profiles predicts clinical outcome in multiple human cancers. *Nat Genet* 38:1043–1048.
- Chang HY, et al. (2004) Gene expression signature of fibroblast serum response predicts human cancer progression: Similarities between tumors and wounds. *PLoS Biol* 2:e7.
- Glinsky GV, Berezovska O, Glinskii AB (2005) Microarray analysis identifies a death-from-cancer signature predicting therapy failure in patients with multiple types of cancer. *J Clin Invest* 115:1503–1521.
- Liu R, et al. (2007) The prognostic role of a gene signature from tumorigenic breast-cancer cells. *N Engl J Med* 356:217–226.
- Paik S, et al. (2004) A multigene assay to predict recurrence of tamoxifen-treated, node-negative breast cancer. *N Engl J Med* 351:2817–2826.
- Rhodes DR, et al. (2004) Large-scale meta-analysis of cancer microarray data identifies common transcriptional profiles of neoplastic transformation and progression. *Proc Natl Acad Sci USA* 101:9309–9314.
- Shiptsin M, et al. (2007) Molecular definition of breast tumor heterogeneity. *Cancer Cell* 11:259–273.
- Sotiriou C, et al. (2006) Gene expression profiling in breast cancer: Understanding the molecular basis of histologic grade to improve prognosis. *J Natl Cancer Inst* 98:262–272.
- van 't Veer LJ, et al. (2002) Gene expression profiling predicts clinical outcome of breast cancer. *Nature* 415:530–536.
- Wang Y, et al. (2005) Gene-expression profiles to predict distant metastasis of lymph node–negative primary breast cancer. *Lancet* 365:671–679.
- Ramaswamy S, Ross KN, Lander ES, Golub TR (2003) A molecular signature of metastasis in primary solid tumors. *Nat Genet* 33:49–54.
- Fan C, et al. (2006) Concordance among gene expression–based predictors for breast cancer. *N Engl J Med* 355:560–569.
- Yager JD, Davidson NE (2006) Estrogen carcinogenesis in breast cancer. *N Engl J Med* 354:270–282.
- Coser KR, et al. (2003) Global analysis of ligand sensitivity of estrogen-inducible and -suppressible genes in MCF7/BUS breast cancer cells by DNA microarray. *Proc Natl Acad Sci USA* 100:13994–13999.
- Bourdeau V, et al. (2008) Mechanisms of primary and secondary estrogen target gene regulation in breast cancer cells. *Nucleic Acids Res* 36:76–93.
- Calvano SE, et al., Inflammation and Host Response to Injury Large-Scale Collaborative Research Program (2005) A network-based analysis of systemic inflammation in humans. *Nature* 437:1032–1037.
- Adler AS, et al. (2006) Genetic regulators of large-scale transcriptional signatures in cancer. *Nat Genet* 38:421–430.
- Bild AH, et al. (2006) Oncogenic pathway signatures in human cancers as a guide to targeted therapies. *Nature* 439:353–357.
- Chuang HY, Lee E, Liu YT, Lee D, Ideker T (2007) Network-based classification of breast cancer metastasis. *Mol Syst Biol* 3:140.
- Rhodes DR, et al. (2007) Molecular concepts analysis links tumors, pathways, mechanisms, and drugs. *Neoplasia* 9:443–454.
- Wong DJ, et al. (2008) Module map of stem cell genes guides creation of epithelial cancer stem cells. *Cell Stem Cell* 2:333–344.
- Musgrove EA, et al. (2008) Identification of functional networks of estrogen- and c-Myc-responsive genes and their relationship to response to tamoxifen therapy in breast cancer. *PLoS One* 3:e2987.
- Cappellen D, Schlange T, Bauer M, Maurer F, Hynes NE (2007) Novel c-MYC target genes mediate differential effects on cell proliferation and migration. *EMBO Rep* 8:70–76.
- Neve RM, et al. (2006) A collection of breast cancer cell lines for the study of functionally distinct cancer subtypes. *Cancer Cell* 10:515–527.
- Hua S, et al. (2008) Genomic analysis of estrogen cascade reveals histone variant H2A.Z associated with breast cancer progression. *Mol Syst Biol* 4:188.
- Grandori C, Cowley SM, James LP, Eisenman RN (2000) The Myc/Max/Mad network and the transcriptional control of cell behavior. *Annu Rev Cell Dev Biol* 16:653–699.
- Minn AJ, et al. (2005) Genes that mediate breast cancer metastasis to lung. *Nature* 436:518–524.
- Irimia D, Toner M (2009) Spontaneous migration of cancer cells under conditions of mechanical confinement. *Integr Biol* 1:506–512.
- Pomerantz MM, et al. (2009) The 8q24 cancer risk variant rs6983267 shows long-range interaction with MYC in colorectal cancer. *Nat Genet* 41:882–884.
- Podsypanina K, et al. (2008) Seeding and propagation of untransformed mouse mammary cells in the lung. *Science* 321:1841–1844.
- Soucek L, et al. (2008) Modeling Myc inhibition as a cancer therapy. *Nature*.
- Trimboli AJ, et al. (2008) Direct evidence for epithelial–mesenchymal transitions in breast cancer. *Cancer Res* 68:937–945.
- Rapp UR, et al. (2009) MYC is a metastasis gene for non–small-cell lung cancer. *PLoS One* 4:e6029.
- D'Cruz CM, et al. (2001) c-MYC induces mammary tumorigenesis by means of a preferred pathway involving spontaneous *Kras2* mutations. *Nat Med* 7:235–239.
- Partanen JI, Nieminen AJ, Mäkelä TP, Klefstrom J (2007) Suppression of oncogenic properties of c-Myc by LKB1-controlled epithelial organization. *Proc Natl Acad Sci USA* 104:14694–14699.
- Zhan L, et al. (2008) Deregulation of scribble promotes mammary tumorigenesis and reveals a role for cell polarity in carcinoma. *Cell* 135:865–878.
- Rhodes DR, et al. (2005) Mining for regulatory programs in the cancer transcriptome. *Nat Genet* 37:579–583.
- Rodriguez-Pinilla SM, et al. (2007) MYC amplification in breast cancer: A chromogenic in situ hybridization study. *J Clin Pathol* 60:1017–1023.
- Robanus-Maandag EC, et al. (2003) Association of C-MYC amplification with progression from the in situ to the invasive stage in C-MYC amplified breast carcinomas. *J Pathol* 201:75–82.
- Benjamini Y, Hochberg Y (1995) Controlling the false discovery rate: A practical and powerful approach to multiple testing. *J R Stat Soc B* 57:289–300.
- McNeil CM, et al. (2006) c-Myc overexpression and endocrine resistance in breast cancer. *J Steroid Biochem Mol Biol* 102:147–155.
- Debnath J, Muthuswamy SK, Brugge JS (2003) Morphogenesis and oncogenesis of MCF-10A mammary epithelial acini grown in three-dimensional basement membrane cultures. *Methods* 30:256–268.